



**HAL**  
open science

## Automated Diagnosis Of Retinal Neovascularization Pathologies From Color Retinal Fundus Images

Rahma Boukadida, Yaroub Elloumi, Rostom Kachouri, Asma Ben Abdallah,  
Mohamed Hedi Bedoui

► **To cite this version:**

Rahma Boukadida, Yaroub Elloumi, Rostom Kachouri, Asma Ben Abdallah, Mohamed Hedi Bedoui. Automated Diagnosis Of Retinal Neovascularization Pathologies From Color Retinal Fundus Images. Computer Graphics International, CGI-2022, Sep 2022, Geneva, Switzerland. 10.1007/978-3-031-23473-6\_35. hal-04006927

**HAL Id: hal-04006927**

**<https://hal.science/hal-04006927>**

Submitted on 27 Feb 2023

**HAL** is a multi-disciplinary open access archive for the deposit and dissemination of scientific research documents, whether they are published or not. The documents may come from teaching and research institutions in France or abroad, or from public or private research centers.

L'archive ouverte pluridisciplinaire **HAL**, est destinée au dépôt et à la diffusion de documents scientifiques de niveau recherche, publiés ou non, émanant des établissements d'enseignement et de recherche français ou étrangers, des laboratoires publics ou privés.

# Automated Diagnosis Of Retinal Neovascularization Pathologies From Color Retinal Fundus Images

Rahma Boukadida <sup>1,2</sup> [0000-0002-5193-4335] Yaroub Elloumi <sup>1,3,4</sup> [0000-0001-8878-7562] Rostom Kachouri <sup>3</sup> [0000-0002-9451-4269]

Asma Ben Abdallah <sup>1</sup> and Mohamed Hedi Bedoui <sup>1</sup> [0000-0002-7443-0543]

<sup>1</sup> Medical Technologie and Image Processing Laboratory , Faculty of Medicine , University of Monastir, Tunisia

<sup>2</sup> Faculty of Sciences of Monastir, University of Monastir, 1002, Tunisia

<sup>3</sup> Gaspard- Monge Computer Science Laboratory , Université Gustave Eiffel CNRS, ESIEE Paris

<sup>4</sup> ISITCom Hammam -Sousse, University of Sousse, Tunisia

rahmaboukadida@yahoo.com

**Abstract.** The retinal Neo-Vascularization (NV) is the abnormal growth of new blood vessels in the retina, which leads to a severe reduction on visual acuity and blindness. It is a main biomarker to screening several diseases, where the Proliferative Diabetic Retinopathy (PDR) and Wet Age-related Macular Degeneration (WAMD) are the most common ones. The NV severity requires a fast screening to avoid severe degradation. However, it is labor intensive and time-consuming for the ophthalmologists.

In this paper, we suggest an automated screening method that automatically detects NV from fundus photography and classify it as PDR, WAMD and Healthy. For this purpose, the image is preprocessed and then provided a transfer learned model of the VGG16 neural network. The method was evaluated using a dataset containing 395 fundus photographs of retinal images where an accuracy of 98.30%, a sensitivity of 98.66%, a specificity of 98.33% were achieved. In addition, the areas under curve in terms of classes were between 98% and 100%.

**Keywords:** Retinal Neovascularization, Wet Age-related Macular degeneration , Proliferative Diabetic Retinopathy, Deep Learning, Transfer Learning.

## 1 Introduction

Neo-Vascularization (NV) is an abnormal formation of new blood vessels, usually in or under the retina. It is caused by a severe lack of oxygen in the retinal capillaries. The new vessels are thin, tortuous and fragile. They may easily start leaking blood on surface of retina and cause severe vision loss, even blindness [1]. NV is associated with a range of ocular disorders, including Age-related Macular Degeneration (AMD), Diabetic Retinopathy (DR), retinopathy of prematurity, corneal neovascularization, retinal vessel occlusion, and neovascular glaucoma. Among these neovascularization-related diseases, AMD and DR are the leading causes of visual impairment in the world [2] which are targeted in this study.

AMD causes severe vision loss in developed countries, particularly in people aged 65 and older. It is considered as the third leading cause of irreversible vision loss worldwide. By 2040, AMD will affect 288 million people worldwide [2]. AMD can be classified into two types. The Dry AMD which is characterized by the appearance of drusens as shown in Fig. 1(b). The Wet AMD (WAMD) occurs due to a Choroidal Neovascularization (CNV) which is an abnormal blood vessel formation from choroid region of the retina, as shown in Fig. 1(c). The WAMD progresses faster and leads to an irreversible loss of sight.

DR is another common cause of human vision loss, which affects actually 463 million people worldwide and 700 million by 2045 [3] [4]. DR has been categorized into two types, Non-proliferative Diabetic Retinopathy (NPDR) and Proliferative Diabetic Retinopathy (PDR). The latter is the most severe stage of DR, which corresponds to 9% of DR affected people [5]. PDR is characterized by neovascularization with or without pre-retinal or vitreal hemorrhages. The detection of PDR in early stage in order to stop or delay its progression leads to avoid vision loss and blindness [6].

The early detection of WAMD and PDR is essential to preserve the visual acuity. The NV, in particular caused by WAMD and PDR, have similar neovascular changes, related to the color and the shape whatever the retinal pathology is. Consequently, it is hard to distinguish between PDR and WAMD. However, misdiagnosis or failure to diagnose results in inadequate medical therapy which leads to severe aggravation of vision and blindness.

In this work, we aim to propose an automated method to differentiate between normal, WAMD and PDR cases through fundus images, in order to save patients from the risk of blindness. Also, it is inexpensive and non-invasive technique and thus, an ideal screening technology to be adopted for the detection of WAMD and PDR.

The paper is organized as follows. Sect. 2 discusses the related work. The suggested method for WAMD and PDR detection is presented in Sect. 3. The evaluation of the proposed method and performance parameters is done in Sect. 4, followed by conclusion in the last section.

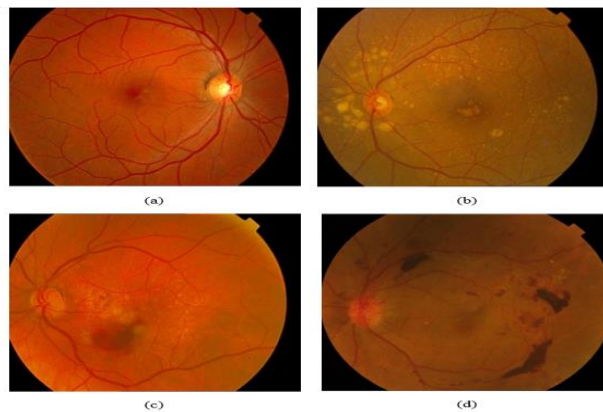


**Fig. 1.** Fundus images : (a) normal , (b) Dry AMD , (c) WAMD , (d) PDR image.

## 2 Related work

Recently, several deep learning systems have been developed for the classification of color fundus photographs into AMD severity scales [7], [8]. These severity scales have included both binary (e.g., Dry vs. WAMD) and multi-class (e.g., the 9-step AREDS Severity Scale and a 4-class AMD classification) systems. The work described by peng et al [9] uses a DL model called « DeepSeeNet », to classify fundus images automatically by the the Age Related Eye Disease Study (AREDS) . Experiment results show that the proposed model achieves an accuracy of 0.671 and a kappa of 0.558 . Grassmann et al. [10] proposed a deep learning based classification architecture to predict the severity of AMD. In this study, an ensemble of several convolutional neural networks was used to classify among 13 different classes of AMD .The experimentation is processed using the AREDS dataset. The accuracy of classifying fundus photographs into 13 different AMD classes was only 63.3% . Keel et al. [11] proposed an algorithm for detecting WAMD based on fundus photography from a private dataset . The work described by Heo et al. [12] developed a DL-based diagnostic tool to detect and differentiate between Dry and WAMD using fundus photographs. The dataset was composed of 399 fundus images. The experimental results show that the proposed model achieves 90.86% accuracy with preprocessing for classification into three classes. Burlina et al. [13] proposed a method a DL algorithm to identify the class of AMD using color fundus photographs from the AREDS. The performances of two-four classes of AMD classification were 93.4%, 81.5%, and 79.4%, respectively.

It is noteworthy that ophthalmologists must distinguish between RDNP and PDR, as the diagnoses have different treatments and prognosis for blindness. There are several works for DR diagnosis at image level based on DL. Pratt et al. [14] proposed a CNN model to evaluate the severity of DR . The classification provides 5 grades such as No DR, Mild DR, Moderate DR, Severe DR and Proliferative DR. EyePACS database was used for training. The proposed model achieved a classification accuracy of 75%. Shanthi et al.[15] present a DL architecture to classify the input into 4 categories. Training and testing were performed, respectively, with 710 and 303 fundus images from the MESSIDOR database. The work described by Riaz et al.[16] presented a CNN for DR classification into 5 classes. The network was implemented on EyePACS/Kaggle and MESSIDOR databases. The performance was evaluated on 1747 images from the MESSIDOR database and 17,978 images from the EyePACS/Kaggle database. Wan et al. [17] evaluated 4 types of CNN architectures to classify DR into 5 categories (0-4). Liu et al.[18] described a challenge named "Diabetic Retinopathy (DR)-Grading and Image Quality Estimation Challenge" in conjunction with ISBI 2020 to hold three sub-challenges and develop deep learning models for DR image assessment and grading. The performance was evaluated using the DeepDRiD dataset containing 2,000 regular DR images and 256 ultra-widefield images. The weighted kappa for DR grading ranged from 0.93 to 0.82. Dai et al.[19] proposed a CNN model to evaluate the severity of DR. Images were obtained from the Shanghai Integrated Diabetes Prevention and Care System study. The grading of diabetic retinopathy as mild, moderate, severe and proliferative achieves area under the curves of 0.943, 0.955, 0.960



### 3.2 Data preprocessing and augmentation

Preprocessing is necessary to make the new vessels visible in a fundus image. The green channel is extracted from the RGB fundus images. This channel is selected because the blood vessels, including those associated with neovascularization, appear clearer in this channel than in the other channels. Then, to improve the visibility of the blood vessels, Contrast Limited Adaptive Histogram Equalization (CLAHE) is used [22] [23]. CLAHE adjusts the contrast of the image in order to ensure that the blood vessels become brighter than the background. The preprocessed images are shown in Figure 3c1, c2, c3. The size of the input retinal images is  $224 \times 224$  pixels.

To increase the diversity of the dataset and improve the robustness of the DL model, we applied data augmentation methods. For this purpose, all images are flipped and shifted horizontally and vertically and rotated with an angle of  $5^\circ$ , as presented in Fig.4.

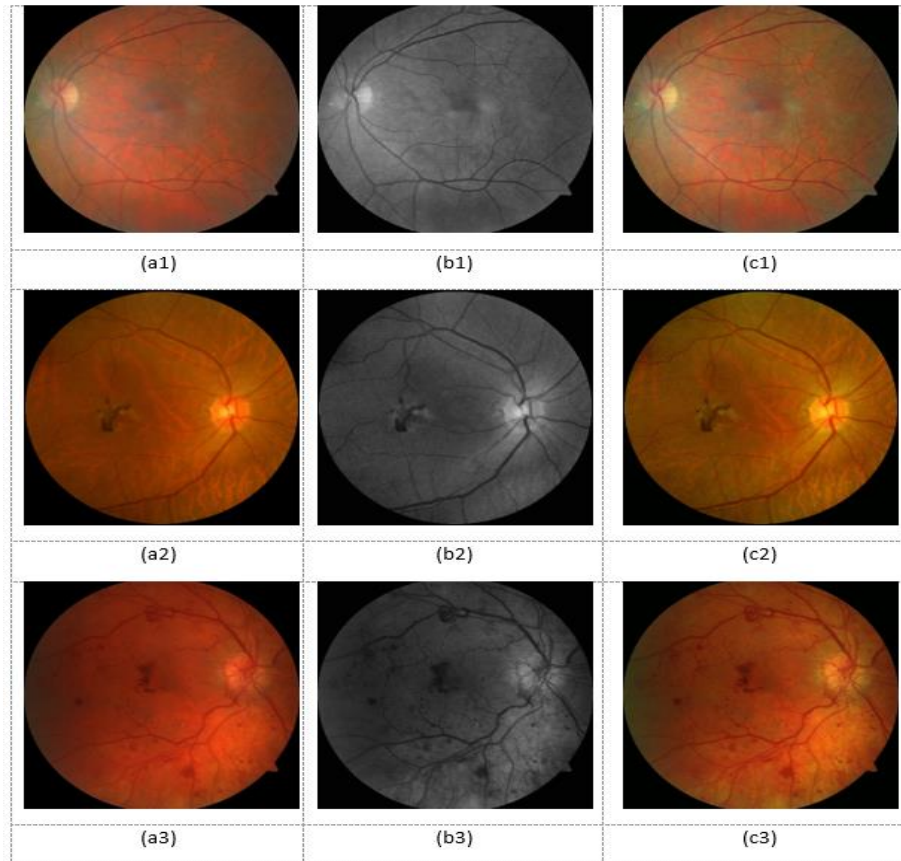


**Fig. 3.** Pre-processing : a1,a2 and a3, healthy , WAMD and PDR image; b1,b2 and b3, green channels of images; c1 ,c2 and c3, pre-processed images

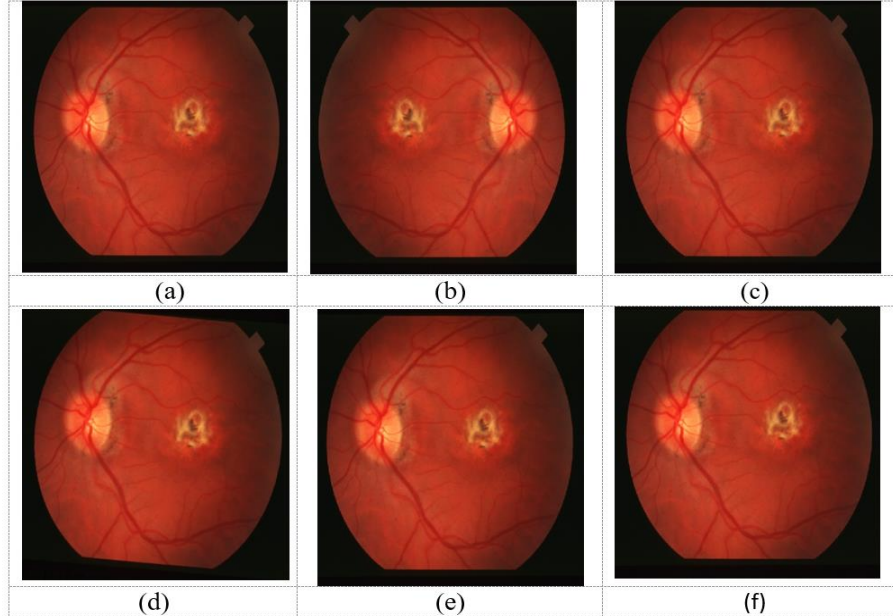


**Fig. 4.** Data augmentation (a) original input, (b) horizontal flip, (c) vertical flip, (e) rotation with  $5^\circ$  of the image, (f) width shift, (g) height shift

### 3.3 Transfer Learning of VGG16 Architecture

In this study, the VGG-16 architecture was applied to achieve transfer learning. VGG-16 is a convolutional neural network by VGGNet (Visual Geometry Group), which was developed by Oxford University Visual Geometry Group researchers to compete in the ImageNet Large-Scale Visual Recognition Challenge (ILSVR) in 2014 [22]. The architecture is composed of 13 convolutional layers, interspersed with 5 pooling layers and ending with 3 dense layers (see Fig 2). The pre-trained CNN model was trained using ImageNet which is a large public dataset that contains 1,000,000 images to be classified into 1,000 classes.

The retinal fundus dataset was utilized to train the pre-trained network, after applying pre-processing on it. To achieve the transfer, the top 2 layers of the pre-trained model, which are employed to classify 1000 classes, were removed and replaced by an a three layers. The first layer is a flatten in order to align all features into a single row. The second layer applies a dropout function to prevent overfitting, with a threshold equal to 0.5. Then , a SoftMax activation function as a classifier with 3 nodes to supply 3 output classes. The new network was re-trained with retinal fundus images dataset with learning rate of 0.00001 .The loss function was minimized using a stochastic gradient descent optimizer with momentum= 0.9. while the number of epochs was 30 epochs. After repeated testing, the batch size was set as 4. The main hyper parameters used for training are summarized in Table 1.

**Table 1.** Table captions should be placed above the tables.

Hyperparameter	Value
Optimizing function	SGD — Stochastic Gradient Descent
Epochs	30
Batch size	4
Learning rate	0.00001
Dropout	0.2
Loss function	categorical cross entropy

## 4 EXPERIMENTAL RESULTS

### 4.1 Dataset

Based on the state of the art study, the databases do not contain enough PDR and WAMD fundus images. For this purpose, we construct a database of 395 images where fundus images are collected from different databases. The dataset contains 115 WAMD images, 114 PDR images and 166 healthy images. The image resources used are collected from four publically accessible databases: ODIR, RFMiD, REFUGE, Dataset from fundus images for the study of DR. The number of images is detailed in Table 2.

ODIR [24]: The Ocular disease intelligent recognition (ODIR) database comprises of pairs of fundus images of 5000 patients labeled for eight categories of ophthalmological diseases. RFMiD [25]: It consists of 3200 fundus images captured using three different fundus cameras with 46 conditions annotated through adjudicated consensus of two senior retinal experts. REFUGE [26]: The REFUGE dataset (Retinal-Fundus-Glaucoma-Challenge) contains 400 fundus images. With 89 AMD images. Dataset from fundus images for the study of DR [27]: This dataset consist of 757 color fundus images acquired at the Department of Ophthalmology of the Hospital de Clínicas, Facultad de Ciencias Médicas (FCM), Universidad Nacional de Asunción (UNA), Paraguay. The acquisition of the retinographies was made through the Visucam 500 camera of the Zeiss brand. Two expert ophthalmologists have classified the dataset.

**Table 2.** Datasets Description

Bases de données	Number of Healthy images	Number of W AMD images	Number of PDR images
ODIR [17]	-	36	-
RFMiD [18]	0	38	0
REFUGE [19]	-	41	0
Dataset from fundus images for the study of DR [20]	166	0	114
Total	166	115	114

## 4.2 Evaluation Metrics

In order to evaluate the performance of our method, we use four parameters, which are sensitivity (Sens), specificity (Spec), accuracy (ACC) and AUC, given in Equations (1)–(3), respectively.

$$\text{Sensitivity} = TP / (TP + FN) \quad (1)$$

$$\text{Specificity} = TN / (TN + FP) \quad (2)$$

$$\text{Accuracy} = (TP + TN) / (TP + TN + FP + FN) \quad (3)$$

where TP, TN, FP and FN are respectively the true positive, the true negative, the false positive and the false negative detected images.

AUC is the area under the Receiver Operating Curve (ROC) and it provides the probability that the model ranks a positive example more highly than a negative example. ROC is a plot between two parameters: True Positive Rate (TPR) and False Positive Rate (FPR). The first is on the Y-axis and the second is on the X-axis. TPR is equal to sensitivity, and FPR is the complement of Specificity. Equation (4) shows the parameter FPR.

$$\text{FPR} = FP / (FP + TN) \quad (4)$$

## 4.3 Performance Evaluation of Proposed Method

The method was developed using the Python language. The pre-processing is executed using the OpenCV library. We trained our model using the "Keras" API. The training and testing steps are executed on the cloud service "google Colab".

The dataset is split where 70% of the data are used for training, 15% for validation and 15% for testing. The accuracy and loss curves on the training and validation set as depicted in Fig.5. The X-axis represents the epoch count, the left Y-axis represents the loss value, and the right Y-axis represents the training accuracy.

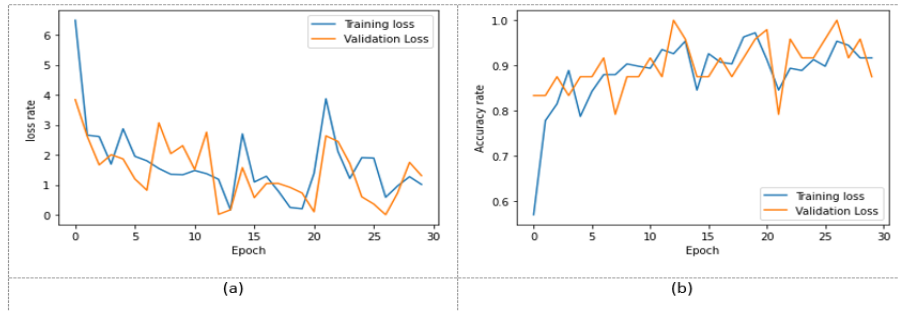


**Fig. 5.** Evaluation of training performance in terms of epochs: (a) Training and validation loss values; (b) Training and validation accuracy values

In addition, the confusion matrix of the test set depicting the true versus the predicted class of 59 fundus images. Fig. 6 shows the confusion matrix. Furthermore, our algorithm successfully identified all fundus images with WAMD and PDR. Thus, 25 images showing a healthy fundus were identified correctly as such, resulting a specificity of 98 % and sensitivity of 96 % for this class. Our results demonstrate that our method is able to differentiate between WAMD and PDR up to 98.30 %. The sensitivity of the system is 98.66 % and the specificity is 98.33 %.

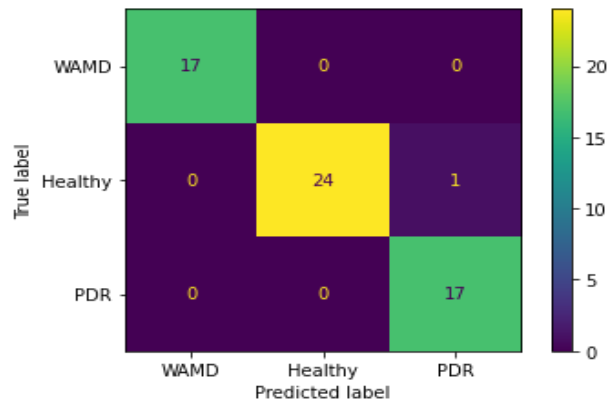


**Fig. 6.** confusion matrix

Figure 7 shows Receiver Operator Characteristic (ROC) curve of each class. The AUC of the model reached 100% , 98% , and 98.81% for detecting WAMD , Healthy images and PDR images .

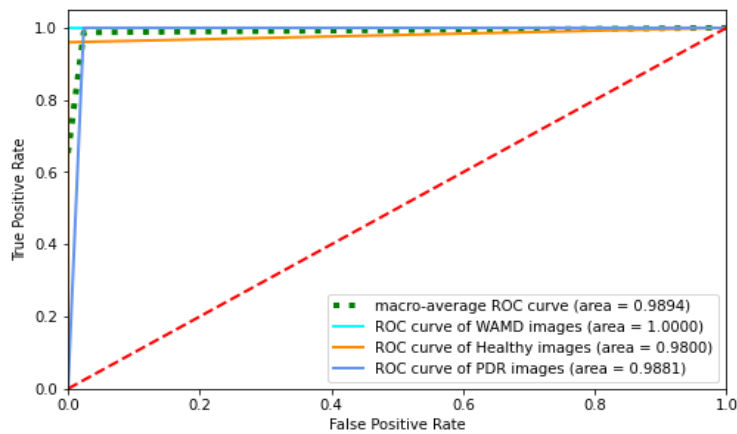


**Fig. 7.** Receiver operating characteristic curves for each class

## 5 Conclusion

PDR and WAMD are common retinal diseases. If not treated timely, they can cause irreversible central vision loss. In this paper, we proposed a diagnostic system for automatic and early identification of WAMD and PDR. For this purpose, we use a deep learning approach based transfer learning with the VGG16 neural network using fundus images. The images of the inputs are directly introduced into the network by processing them in advance. The images are preprocessed and resized. The data augmentation is used to increase the data set. The main features used to detect diseases are extracted automatically.

The experimental results demonstrate the reliability of the proposed method. Our proposed method has achieved an ACC of 98.30%, a sensitivity of 98.66%, a specificity of 98.33% and a AUC of 98.94%. Further, the results suggest that this method may provide an efficient, cost-effective and precise diagnosis of healthy, PDR and WAMD fundus images. Hence proper treatment can be provided to impede the progression of the diseases. Also, this method is the first attempt to differentiate fundus images into normal, dry AMD, and wet AMD classes. Furthermore, this suggested contribution is able to be implemented into a mobile End-To-End system for retinal pathology screening [28], [29].

## References

1. S. Yu, D. Xiao, et Y. Kanagasiam, « Machine Learning Based Automatic Neovascularization Detection on Optic Disc Region », *IEEE J. Biomed. Health Inform.*, vol. 22, n° 3, p. 886-894, mai 2018, doi: 10.1109/JBHI.2017.2710201.
2. W. L. Wong *et al.*, « Global prevalence of age-related macular degeneration and disease burden projection for 2020 and 2040: a systematic review and meta-analysis », *The Lancet Global Health*, vol. 2, n° 2, p. e106-e116, févr. 2014, doi: 10.1016/S2214-109X(13)70145-1.
3. « International Diabetes Federation. International diabetes federation diabetes atlas ». <https://www.diabetesatlas.org/en/>
4. Y. Elloumi, N. Abroug, et M. H. Bedoui, « End-to-End Mobile System for Diabetic Retinopathy Screening Based on Lightweight Deep Neural Network », in *Advances in Intelligent Data Analysis XX*, vol. 13205, T. Bouadi, E. Fromont, et E. Hüllermeier, Éd. Cham: Springer International Publishing, 2022, p. 66-77. doi: 10.1007/978-3-031-01333-1\_6.
5. R. Boukadida, Y. Elloumi, M. Akil, et M. H. Bedoui, « MOBILE-AIDED screening system for proliferative diabetic retinopathy », *Int J Imaging Syst Technol*, vol. 31, n° 3, p. 1638-1654, sept. 2021, doi: 10.1002/ima.22547.
6. Y. Elloumi, M. Ben Mbarek, R. Boukadida, M. Akil, et M. H. Bedoui, « Fast and accurate mobile-aided screening system of moderate diabetic retinopathy », in *Thirteenth International Conference on Machine Vision*, Rome, Italy, janv. 2021, p. 93. doi: 10.1117/12.2588505.

7. S. B. Sayadia, Y. Elloumi, R. Kachouri, M. Akil, A. B. Abdallah, et M. H. Bedoui, « Automated method for real-time AMD screening of fundus images dedicated for mobile devices », *Med Biol Eng Comput*, vol. 60, n° 5, p. 1449-1479, mai 2022, doi: 10.1007/s11517-022-02546-8.
8. Y. Elloumi, M. Akil, et H. Boudegga, « Ocular diseases diagnosis in fundus images using a deep learning: approaches, tools and performance evaluation », in *Real-Time Image Processing and Deep Learning 2019*, Baltimore, United States, mai 2019, p. 30. doi: 10.1117/12.2519098.
9. Y. Peng *et al.*, « DeepSeeNet: A Deep Learning Model for Automated Classification of Patient-based Age-related Macular Degeneration Severity from Color Fundus Photographs », *Ophthalmology*, vol. 126, n° 4, p. 565-575, avr. 2019, doi: 10.1016/j.ophtha.2018.11.015.
10. F. Grassmann *et al.*, « A Deep Learning Algorithm for Prediction of Age-Related Eye Disease Study Severity Scale for Age-Related Macular Degeneration from Color Fundus Photography », *Ophthalmology*, vol. 125, n° 9, p. 1410-1420, sept. 2018, doi: 10.1016/j.ophtha.2018.02.037.
11. S. Keel *et al.*, « Development and validation of a deep-learning algorithm for the detection of neovascular age-related macular degeneration from colour fundus photographs », *Clin Experiment Ophthalmol*, vol. 47, n° 8, p. 1009-1018, nov. 2019, doi: 10.1111/ceo.13575.
12. T.-Y. Heo *et al.*, « Development of a Deep-Learning-Based Artificial Intelligence Tool for Differential Diagnosis between Dry and Neovascular Age-Related Macular Degeneration », *Diagnostics*, vol. 10, n° 5, p. 261, avr. 2020, doi: 10.3390/diagnostics10050261.
13. P. Burlina, K. D. Pacheco, N. Joshi, D. E. Freund, et N. M. Bressler, « Comparing humans and deep learning performance for grading AMD: A study in using universal deep features and transfer learning for automated AMD analysis », *Computers in Biology and Medicine*, vol. 82, p. 80-86, mars 2017, doi: 10.1016/j.combiomed.2017.01.018.
14. H. Pratt, F. Coenen, D. M. Broadbent, S. P. Harding, et Y. Zheng, « Convolutional Neural Networks for Diabetic Retinopathy », *Procedia Computer Science*, vol. 90, p. 200-205, 2016, doi: 10.1016/j.procs.2016.07.014.
15. T. Shanthi et R. S. Sabeenian, « Modified Alexnet architecture for classification of diabetic retinopathy images », *Computers & Electrical Engineering*, vol. 76, p. 56-64, juin 2019, doi: 10.1016/j.compeleceng.2019.03.004.
16. H. Riaz, J. Park, H. Choi, H. Kim, et J. Kim, « Deep and Densely Connected Networks for Classification of Diabetic Retinopathy », *Diagnostics*, vol. 10, n° 1, p. 24, janv. 2020, doi: 10.3390/diagnostics10010024.
17. S. Wan, Y. Liang, et Y. Zhang, « Deep convolutional neural networks for diabetic retinopathy detection by image classification », *Computers & Electrical Engineering*, vol. 72, p. 274-282, nov. 2018, doi: 10.1016/j.compeleceng.2018.07.042.
18. R. Liu *et al.*, « DeepDRiD: Diabetic Retinopathy—Grading and Image Quality Estimation Challenge », *Patterns*, vol. 3, n° 6, p. 100512, juin 2022, doi: 10.1016/j.patter.2022.100512.
19. L. Dai *et al.*, « A deep learning system for detecting diabetic retinopathy across the disease spectrum », *Nat Commun*, vol. 12, n° 1, p. 3242, déc. 2021, doi: 10.1038/s41467-021-23458-5.

20. H. Ghebrechristos, G. Alaghband, et R. Y. Hwang, « RetiNet — Feature Extractor for Learning Patterns of Diabetic Retinopathy and Age-Related Macular Degeneration from Publicly Available Datasets », in *2017 International Conference on Computational Science and Computational Intelligence (CSCI)*, Las Vegas, NV, USA, déc. 2017, p. 1643-1648. doi: 10.1109/CSCI.2017.286.
21. C. González-Gonzalo *et al.*, « Evaluation of a deep learning system for the joint automated detection of diabetic retinopathy and age-related macular degeneration », *Acta Ophthalmol*, vol. 98, n° 4, p. 368-377, juin 2020, doi: 10.1111/aos.14306.
22. K. Simonyan et A. Zisserman, « Very Deep Convolutional Networks for Large-Scale Image Recognition », 2014, doi: 10.48550/ARXIV.1409.1556.
23. H. Boudegga, Y. Elloumi, M. Akil, M. Hedi Bedoui, R. Kachouri, et A. B. Abdallah, « Fast and efficient retinal blood vessel segmentation method based on deep learning network », *Computerized Medical Imaging and Graphics*, vol. 90, p. 101902, juin 2021, doi: 10.1016/j.compmedimag.2021.101902.
24. « OIA-ODIR ». [En ligne]. Disponible sur: <https://odir2019.grand-challenge.org>
25. « RFMid ». <https://riadd.grand-challenge.org/download-all-classes/>
26. « refuge-AMD ». <https://refuge.grand-challenge.org/iChallenge-AMD/>
27. V. E. Castillo Benítez *et al.*, « Dataset from fundus images for the study of diabetic retinopathy », *Data in Brief*, vol. 36, p. 107068, juin 2021, doi: 10.1016/j.dib.2021.107068.
28. Y. Elloumi, « Cataract grading method based on deep convolutional neural networks and stacking ensemble learning », *Int J Imaging Syst Tech*, vol. 32, n° 3, p. 798-814, mai 2022, doi: 10.1002/ima.22722.
29. Y. Mrad, Y. Elloumi, M. Akil, et M. H. Bedoui, « A Fast and Accurate Method for Glaucoma Screening from Smartphone-Captured Fundus Images », *IRBM*, p. S1959031821000725, juin 2021, doi: 10.1016/j.irbm.2021.06.004.